

# Hydration and Strength of High Performance Concrete

Bertil Persson

*Division Building Materials, Lund Institute of Technology, Lund, Sweden*

*In this article an experimental and numerical study on the hydration, internal relative humidity, and strength of high performance concrete is outlined. For this purpose about 650 cores were drilled out of 24 simulated columns which had a diameter of 1 m. Eight mixed proportions of concrete were studied. The specimens were air-cured, sealed, or water-cured. Both compressive strength and split tensile strength were studied. Parallel strength tests were carried out on cubes that were made of concrete from the same batch of concrete as the columns. The fragments from the strength tests were used to observe the hydration. The internal relative humidity was measured in about 150 cast-in pipes at different distances from the exposed surface of the column. The study was carried out over a period of 450 days but the specimens are still available for future research.* ADVANCED CEMENT BASED MATERIALS 1996, 3, 107–123

**KEY WORDS:** Compressive strength, Concrete, Cylinder strength, High performance concrete, High strength concrete, Hydration, Internal relative humidity, Moisture, Self-desiccation, Split tensile strength, Strength, Tensile strength

**H**igh performance concrete (HPC) stands for a concrete with a 28-day 100-mm cube compressive strength exceeding 80 MPa. HPC has good rheological properties. In a fresh state, it is possible to mix, transport, and cast HPC with existing methods. The maximum compressive strength will be about 180 MPa in these conditions. Because such a concrete possesses, in addition to high strength, several other favorable qualities such as low permeability and self-desiccation, it was designated high performance concrete.

The water/cement ( $w/c$ ) ratio in the concrete is greater than 0.38 for a normal concrete, whereas it varies between 0.20 and 0.38 for HPC. The low  $w/c$  ratio requires special additives in the concrete silica fume and, above all, a superplasticizer to obtain good work-

ability. Usually special cements are also required. The type of aggregate is important to obtain high strength. The grading of the aggregate influences the workability. The order in which the materials are mixed is also important for the workability of the concrete. Several properties of the concrete are firmly related to the  $w/c$  ratio, such as compressive strength, internal relative humidity, hydration, and creep compliance. Other properties such as Young's modulus, Poisson's ratio, and the creep coefficient do not vary much as compared to normal concrete, because they are mainly dependent on the quality of the aggregate.

## Objective of the Work

The main objective of this work was to investigate the long-term strength of HPC subjected to different external conditions, such as air or water, by observing its compressive and tensile strength, hydration, and self-desiccation. As a reference, studies were carried out on membrane-cured specimens. The effect of silica fume on the strength was of interest. An experimental comparison with the properties of normal concrete was made. The work was carried out between 1989 and 1992. It was financed by the Swedish Council of Technological Development, NUTEK. This article contains only original results.

## Design of Specimens

It was essential to design a specimen consisting of as large a homogeneous concrete as possible. Each batch consisted of 250 kg concrete. The weight of the specimen was 200 kg. The specimen simulated a circular column 1 m in diameter but only 100 mm long. Twenty-four specimens were manufactured (about 5 tons). In Figure 1, details of the specimens are given. In fabricating the specimen, the following detailed program was followed:

1. The gravel contained about 4% moisture calculated on the dry weight of the gravel.

Address correspondence to: Bertil Persson, Division Building Materials, Lund Institute of Technology, Box 118, S-22100 Lund, Sweden.

Received March 11, 1994; Accepted January 1, 1996

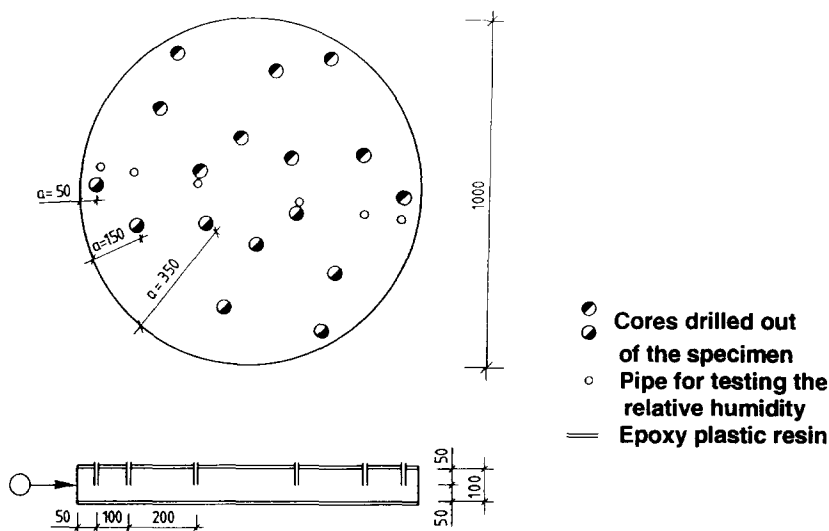


FIGURE 1. Plan and section of specimen.

TABLE 1. Chemical composition of cement [1]

| Component                      | %                      |
|--------------------------------|------------------------|
| Analyzed properties            |                        |
| CaO                            | 64.6                   |
| SiO <sub>2</sub>               | 21.8                   |
| Al <sub>2</sub> O <sub>3</sub> | 3.34                   |
| Fe <sub>2</sub> O <sub>3</sub> | 4.39                   |
| MgO                            | 0.84                   |
| K <sub>2</sub> O               | 0.62                   |
| Na <sub>2</sub> O              | 0.07                   |
| Alkali                         | 0.48                   |
| SO <sub>3</sub>                | 2.23                   |
| CO <sub>2</sub>                | 0.14                   |
| Ignition losses                | 0.63                   |
| Free CaO                       | 1.13                   |
| Mineralogical properties       |                        |
| C <sub>2</sub> S               | 22.5                   |
| C <sub>3</sub> S               | 53.0                   |
| C <sub>3</sub> A               | 1.42                   |
| C <sub>4</sub> AF              | 13.4                   |
| Physical properties            |                        |
| Blaine                         | 325 m <sup>2</sup> /kg |
| Density                        | 3180 kg/m <sup>3</sup> |

2. All materials except for the water and the superplasticizer were then mixed for 30 seconds.
3. The water was added and mixed for another 30 seconds.
4. As a final stage of the mixing procedure, the superplasticizer was added and mixed for 3 minutes.
5. The concrete was poured into a steel mold and vibrated for 2 minutes.
6. The specimen was membrane-cured for 16 hours and then demolded.
7. The flat sides of the specimen were insulated with 2-mm epoxy resin to retain the moisture.
8. The rim on one third of the specimens was treated with 2-mm epoxy (membrane curing).
9. The curing of the rim of the specimens started 3 days after casting (air or water curing).

## Tested Concretes

A low-alkali cement was used. The chemical composition of the cement is shown in Table 1. The aggregate consisted of crushed quartzite sandstone 8–12 mm

TABLE 2. Composition (kg/m<sup>3</sup>) and properties in fresh state of the concretes [1]

| Littera                 | 1     | 2     | 3     | 4     | 5     | 6     | 7     | 8     |
|-------------------------|-------|-------|-------|-------|-------|-------|-------|-------|
| Quartzite               | 1358  | 1145  | 1150  | 1153  | 1214  | 1158  | 1306  | 1306  |
| Gravel                  | 525   | 812   | 846   | 825   | 723   | 730   | 630   | 549   |
| Cement, C               | 484   | 299   | 303   | 298   | 400   | 389   | 456   | 476   |
| Silica fume, S          | 48    |       |       | 30    |       | 39    |       | 48    |
| Superplasticizer        | 13.32 |       | 3.01  | 2.13  | 3.35  | 3.07  | 8.84  | 7.78  |
| Density                 | 2533  | 2424  | 2441  | 2451  | 2469  | 2456  | 2513  | 2500  |
| Water/cement ratio, w/c | 0.222 | 0.577 | 0.465 | 0.483 | 0.326 | 0.358 | 0.251 | 0.243 |
| Air content (%)         | 0.95  | 0.75  | 1.1   | 0.95  | 1.4   | 1.1   | 1.5   | 0.8   |
| Workability (vebe)      | 29    | 15    | 9     | 12    | 25    | 12    | 34    | 13    |
| Aggregate content       | 0.712 | 0.738 | 0.753 | 0.746 | 0.731 | 0.712 | 0.731 | 0.700 |

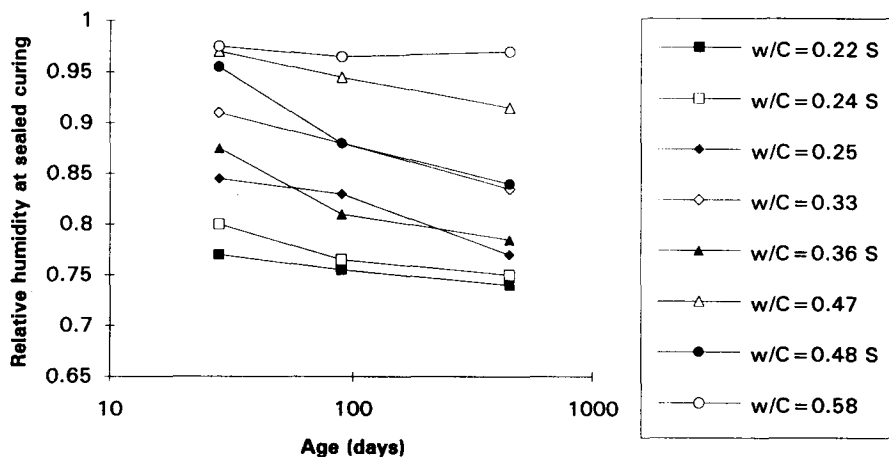


**FIGURE 2.** Relative humidity at sealed curing as a function of logarithmic age. The w/c ratio (w/C) is given in the figure. S = 10% silica fume.

(compressive strength, 333 MPa; split tensile strength, 15 MPa; Young's modulus, 60 GPa; ignition losses, 0.25%) together with natural gravel 0-8 mm (granite, ignition losses, 0.85%) [1,2]. The silica fume was granulated (ignition losses, 2.25%) [1]. The superplasticizer was naphthalene sulfonate. Half of the concretes contained silica fume. As a reference, some normal concretes were made. In Table 2, the composition ( $\text{kg}/\text{m}^3$  dry material) of the concretes and the properties in fresh state are stated.

## Internal Relative Humidity

The moisture conditions in the concrete affect both the mechanical properties and the hydration of the cement. It was thus essential to examine the internal relative humidity of the concrete. The internal relative humidity,  $\phi$ , of the concrete was measured by two sensors at a distance of 50, 150, and 250 mm from the edge of the rim. For the epoxy-treated edges of the specimens, the  $\phi$  was observed at six different locations in each concrete.

The sensors were calibrated for 22 hours before and after each measurement, according to ASTM E 104-85 [3]. The period of measurement was 22 hours. The sensor was placed in a case in plastic pipe in the concrete. A rubber membrane made it possible to seal to prevent moisture losses between the pipe and the sensor. The temperature of the sensor as well as that of the concrete was 20°C. The accuracy of the measurement was within 2%  $\phi$ . In Figure 2, the development of the internal relative humidity during sealed curing is given as a function of logarithmic age (mean value of six measurements each). In Figure 3 and Figure 4, the relative humidity at a distance of 50 mm from the exposed edge of the rim is given as function of age for air curing and water curing, respectively (mean value of two measurements each). The self-desiccation of the HPC was remarkably high even as close as 50 mm from the exposed surface of the rim. In Figure 5,  $\phi$  at sealed curing is given as a function of the w/c ratio (mean value of six measurements each). From Figure 5, the following relationships between the internal relative humidity,  $\phi$ , at sealed condition and the w/c ratio in concrete was evaluated:

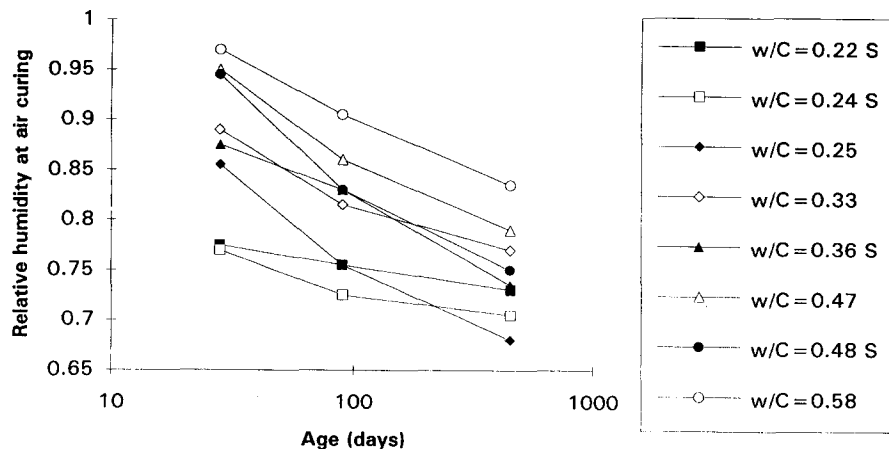


**FIGURE 3.** Relative humidity at air curing 50 mm from the edge of the rim. The w/c ratio (w/C) is given in the figure. S = 10% silica fume.

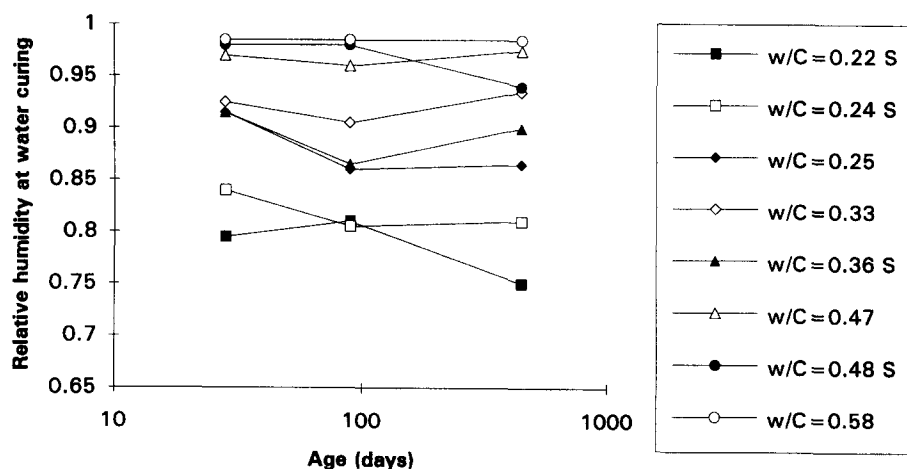


**FIGURE 4.** Relative humidity at water curing 50 mm from the edge of the rim. The w/c ratio (w/C) is given in the figure. S = 10% silica fume.

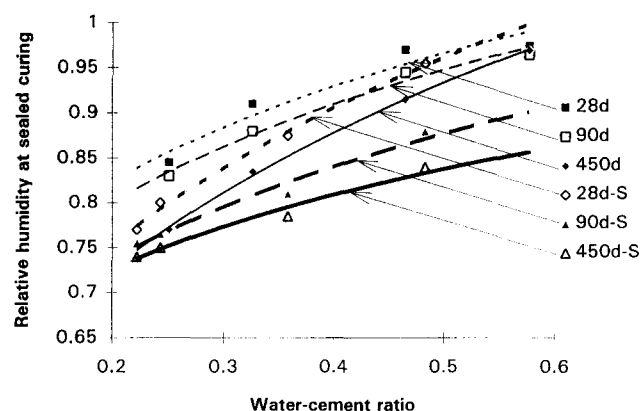


**FIGURE 5.** Relative humidity at sealed curing as a function of the w/c ratio. The age is given in the figure. S = 10% silica fume.

$$\phi = 1.08 \times (1 + 0.0001 \times t) \times (w/c)^{0.16 \times (1 + 0.0015 \times t)} \quad \{\text{without silica fume, } R^2 = 0.93\} \quad (1)$$

$$\phi = 1.39 \times (1 - 0.056 \times \ln t) \times (w/c)^{0.38 \times (1 - 0.1 \times \ln t)} \quad \{10\% \text{ silica fume, } R^2 = 0.90\} \quad (2)$$

where  $t$  is the age of concrete (days) and  $R^2$  is the coefficient of variation.

## Strength Development

The tested objects consisted of cores of 40 mm diameter drilled out of the large specimen. At 28 days, 90 days, and 450 days each, 3 cores were drilled out of the rim at a distance of 50 mm from the exposed edge. Three cores were taken out 150 mm from the edge and 3 cores were taken at 250 mm from the edge. In all, 648 cores were used. After the cores were drilled out, the holes were filled with sand and tightened with epoxy plastic resin. The cores were cut and ground to a length of 80 mm. The cores were weighed and measured before the strength was tested. One third of the specimens were used to obtain the split tensile strength. The remaining

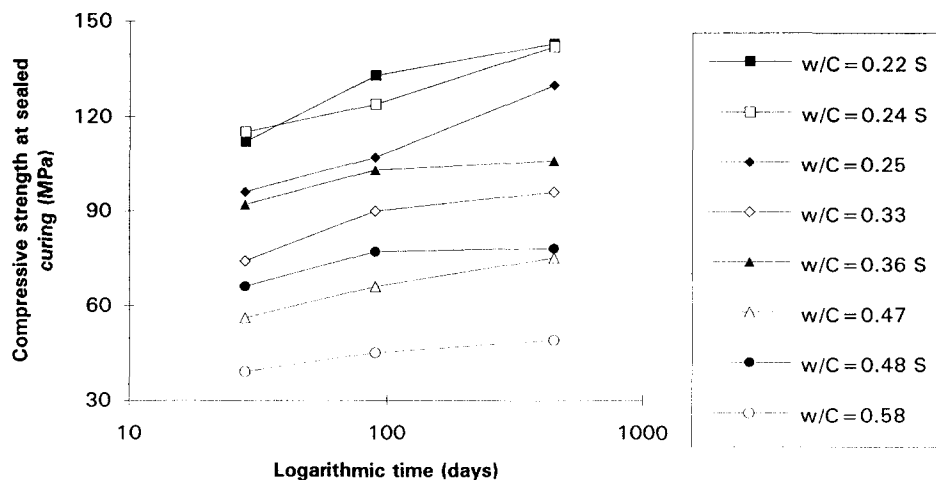


**FIGURE 6.** Compressive strength at sealed curing as a function of the age. The w/c ratio (w/C) is given. S = 10% silica fume.

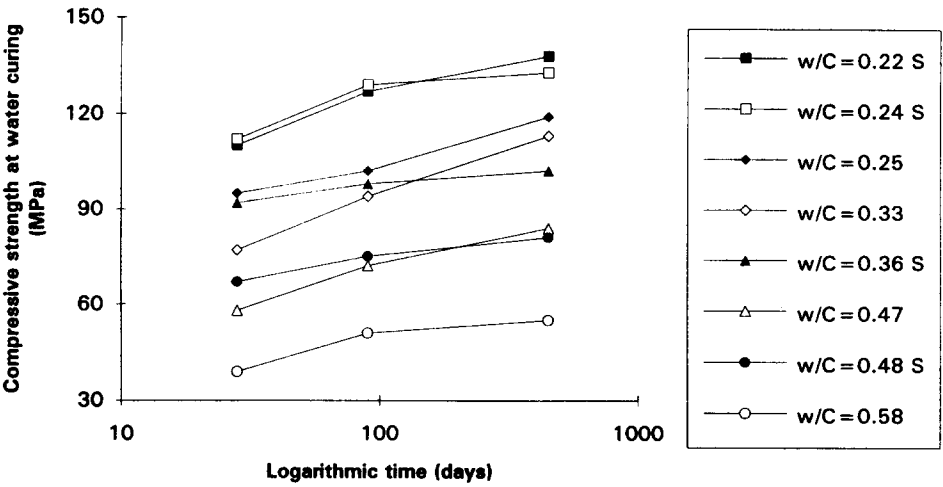


**FIGURE 7.** Compressive strength at water curing as a function of the age. The w/c ratio (w/C) is given. S = 10% silica fume.

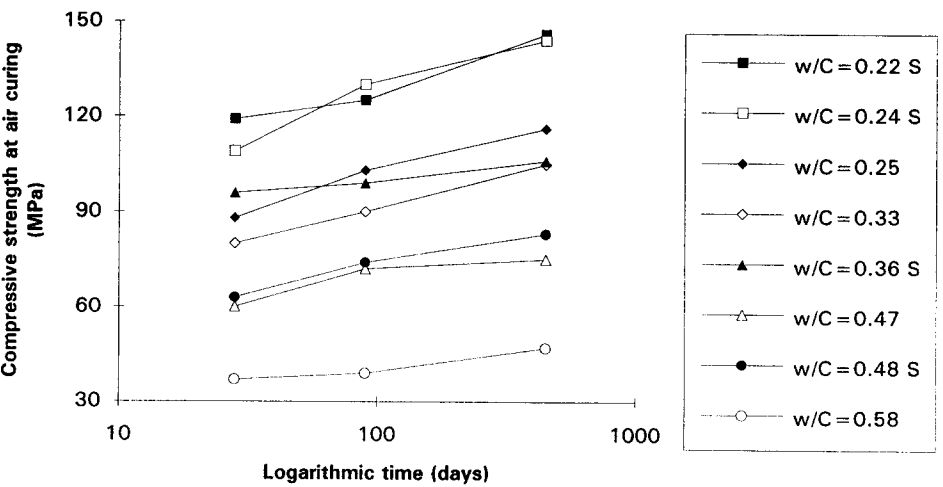


**FIGURE 8.** Compressive strength at air curing as a function of the age. The w/c ratio (w/C) is given. S = 10% silica fume.

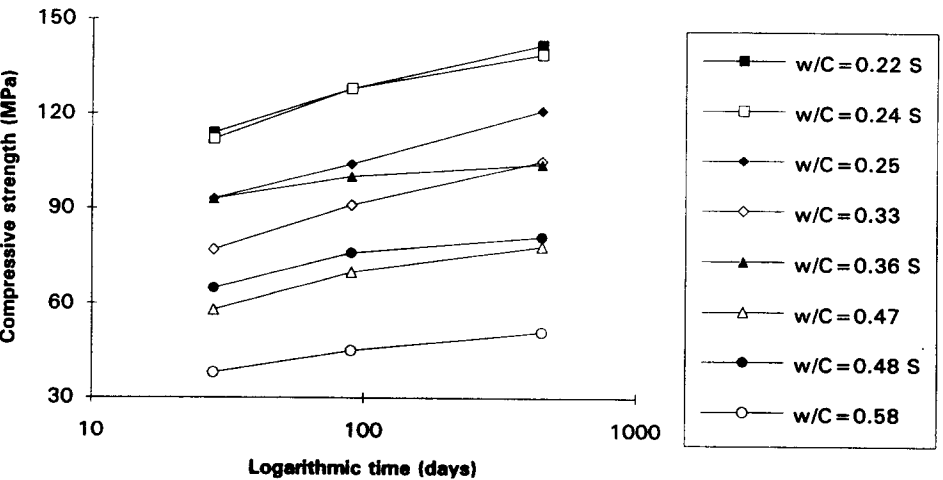


**FIGURE 9.** Average compressive strength as a function of the age. The w/c ratio (w/C) is given. S = 10% silica fume.

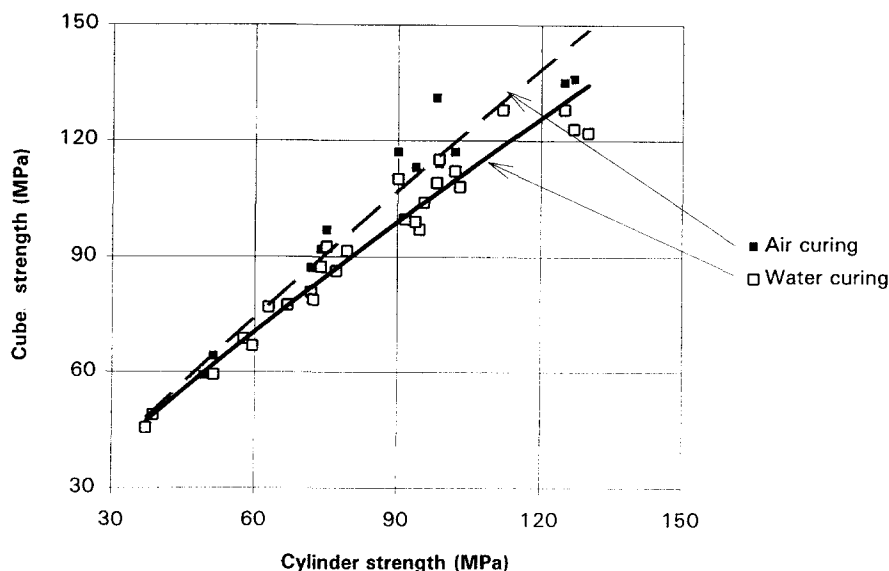


**FIGURE 10.** Cube strength as a function of the cylinder strength at air curing or water curing.

cores were used to obtain the compressive strength. The compressive stress was applied at a rate of 1 MPa/s. Interlayers of 5-mm hardboard were placed between the concrete and the pressure plates of the testing machine. The width of the interlayers of hardboard when obtaining the split tensile strength was 3.5 mm. The ultimate split stress was applied for a duration of at least 30 seconds. In Figures 6, 7, and 8, the compressive strength at membrane curing, air curing, and water curing is shown as a function of age. Each mark corresponds to the mean value of the compressive strength of 6 cores. The difference in the strength due to the kind of curing was very little, probably due to the large size of the specimen. In Figure 9, the mean value of the compressive strength at distances of 50, 150, and 350 mm from the edge is shown as a function of the age. Each mark then corresponds to 18 cores tested.

The compressive strength in all 72 cubes, 28 days or 90 days of age, was tested on concretes from the same

batches as the cores [1]. The same kind of 5-mm hardboard interlayers was used between the concrete and the testing device as for the cores. The development of the strength of air-cured or water-cured 150-mm cubes is given in Figure 10 as a function of the cylinder strength of 40-mm cylinder cores, either air or water cured.

## Analysis of Compressive Strength

From Figure 10, the following expressions were obtained between the cube strength and the cylinder strength of HPC (MPa):

$$f_{ccb,air} = 1.86 \times f_{cc}^{0.9} \quad \{R^2 = 0.95\} \quad (3)$$

$$f_{ccb,wat} = 2.32 \times f_{cc}^{0.83} \quad \{R^2 = 0.97\} \quad (4)$$

where  $f_{ccb,air}$  is the compressive strength of 150 mm cubes cured in air (MPa),  $f_{cc}$  is the strength of cylinders;

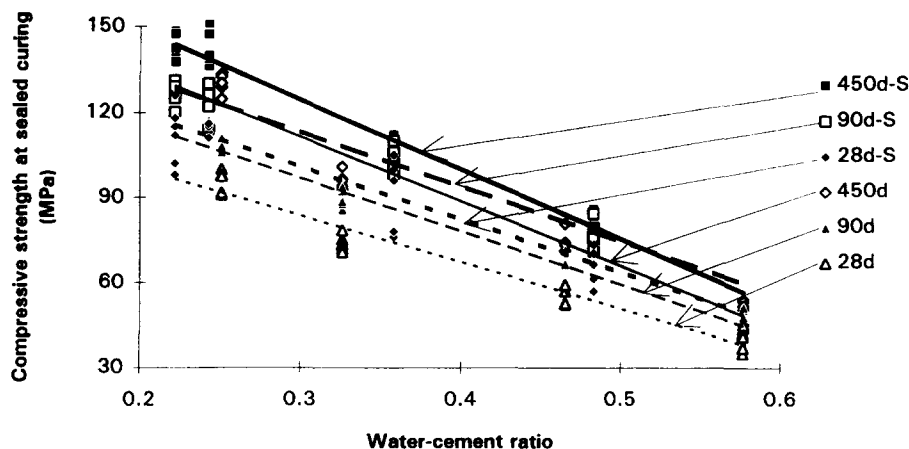


**FIGURE 11.** Compressive strength of 144 cores at sealed curing as a function of the w/c ratio at different ages. d = days; S = 10% silica fume.

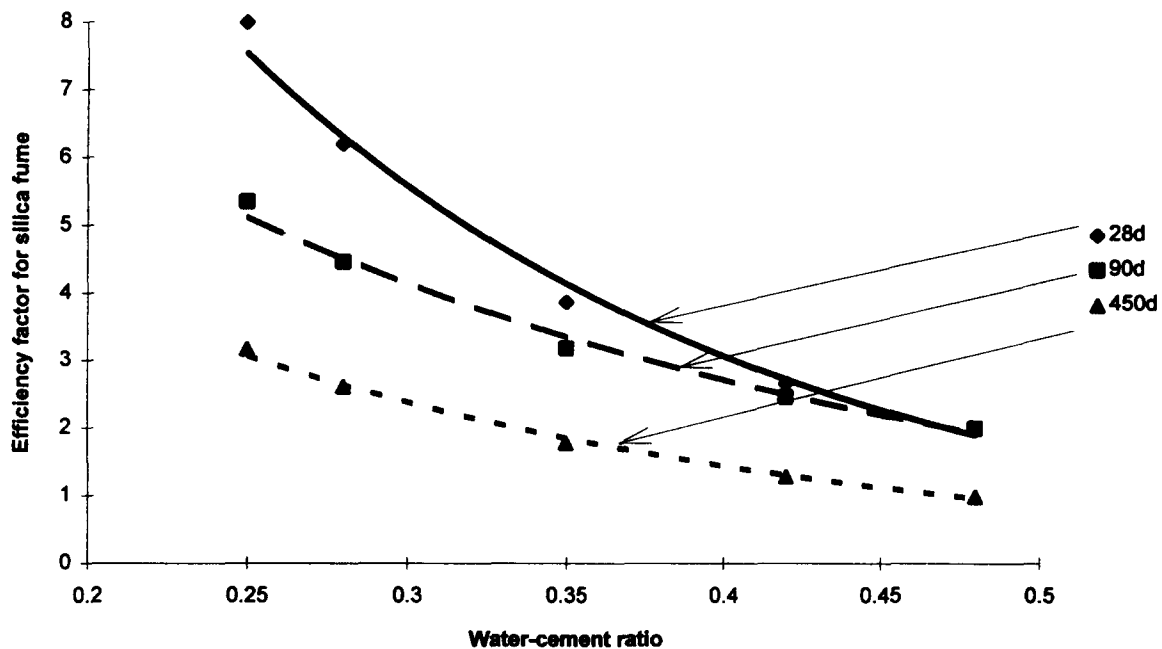


**FIGURE 12.** Efficiency factor for silica fume related to strength according to eq 5 as a function of the w/c ratio at different ages of the concrete. d = days.

80 mm in length and with a diameter of 40 mm (MPa),  $f_{ccb,wat}$  is the compressive strength of 150 mm cubes cured in water (MPa), and  $R^2$  is the coefficient of variation.

The effect of the kind of curing was more or less the same for HPC as for normal concrete. It was therefore of more interest to study the effect of age, or w/c ratio, and of silica fume on the strength of the HPC. In Figure 11, a summary is given of the compressive strength of 144 cores as a function of the w/c ratio at different ages. The content of silica fume is given.

It was appropriate to define the effective water/binder ratio,  $wbr_{eff}$ :

$$wbr_{eff} = w / (c + k_s \times S) \quad (5)$$

where  $w$  is the water content in the concrete ( $\text{kg}/\text{m}^3$ ),  $c$  is the cement content in the concrete ( $\text{kg}/\text{m}^3$ ),  $k_s$  is the

efficiency factor of silica fume related to the compressive strength of the concrete, and  $S$  is the content of silica fume ( $\text{kg}/\text{m}^3$ ).

From Figure 11 the following expression was obtained for the compressive strength (MPa):

$$f_{cc} = 16.9 \times [4.55 - 5.08 \times wbr_{eff} + (1 - 1.36 \times wbr_{eff}) \times \ln t] \quad (R^2 = 0.95) \quad (6)$$

where  $f_{cc}$  is the strength of cylinders that are 80 mm in length and with a diameter of 40 mm (MPa),  $wbr_{eff}$  is the effective water/binder ratio defined in eq 5, and  $t$  is age (days).

The efficiency factor was dependent on age and on w/c ratio according to Figure 12. The efficiency factor was astonishingly large at 28 days age, especially at a

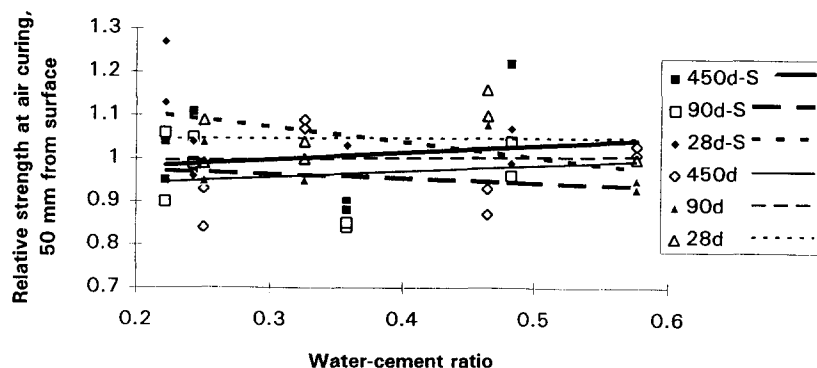


**FIGURE 13.** Relative strength at air curing (ratio of strength at air curing and strength at sealed curing), 55 mm from the surface as a function of the w/c ratio. d = days; S = 10% silica fume.

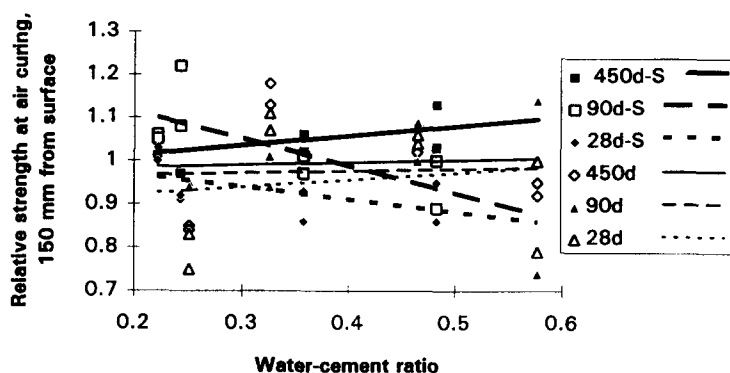


FIGURE 14. Relative strength at air curing, 150 mm from the surface as a function of the w/c ratio. d = days; S = 10% silica fume.

lower w/c ratio. However, the long-term effect of silica fume decreased to less than half at 450 days of age compared with the effect at 28 days. The strength increase of an HPC with silica fume was much lower than the strength increase in a concrete without silica fume, which explained the development of the efficiency factor. Equation 7 gives the efficiency factor:

$$k_s = 112 \times t^{-0.40} \times e^{(0.00073 \times t - 5.23) \times w/c} \{R^2 = 0.99\} \quad (7)$$

where  $k_s$  is the efficiency factor of silica fume related to the compressive strength of the concrete according to Eq 5,  $w$  is the water content in the concrete ( $\text{kg}/\text{m}^3$ ),  $c$  is the cement content in the concrete ( $\text{kg}/\text{m}^3$ ),  $t$  is age (days),  $R^2$  is the coefficient of variation, and  $e$  is the natural logarithm

## Effect of Air Curing or Water Curing on Cylinder Strength

The effect of air curing or water curing on the cube strength was studied earlier. As expected, a minor increase in strength was observed when the surface of the concrete cube dried at air curing. The opposite effect on the compressive strength was observed when the concrete was water cured. One of the objectives of the work was to study the effect on the strength due to the dis-

tances to the surface of the concrete. In Figure 13, the relative strength at air curing (ratio of strength at air curing and strength at sealed curing) 50 mm from the surface is given as a function of the w/c ratio. In Figure 14, the relative strength at air curing 150 mm from the surface is given as a function of the w/c ratio. In Figure 15, the relative strength at air curing 350 mm from the surface is given as a function of the w/c ratio. The effect of the air curing was less than 10% of the relative strength irrespective of the distance to the surface of the specimen. Only tendencies could be observed on concretes with higher w/c ratio (normal concrete): a slight increase of the strength at air curing, 50 mm from the surface. At lower w/c ratio, no long-term effects on the strength of the air curing could be observed. The reason for the small differences was the size of the specimen; it simulated a column, 1 m in diameter.

Figure 16 shows the relative strength at water curing (ratio of strength at water curing and strength at sealed curing), 50 mm from the surface, as a function of the w/c ratio. In Figure 17, the relative strength at water curing 150 mm from the surface is given as a function of the w/c ratio. In Figure 18, the relative strength at water curing 350 mm from the surface is shown as a function of the w/c ratio. At water curing, the compressive strength of a normal concrete increased more than 30% at a distance of 50 mm from the surface provided the concrete did not contain silica fume. If 10% silica fume

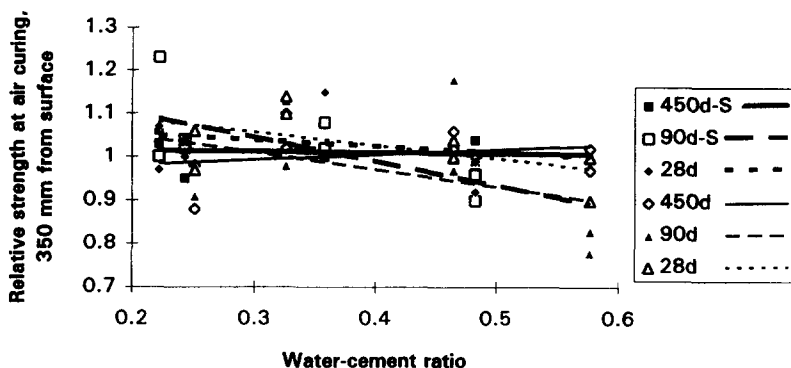
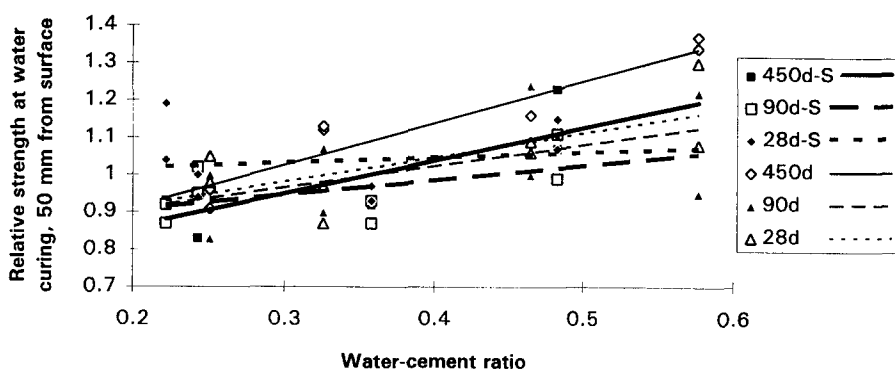


FIGURE 15. Relative strength at air curing, 350 mm from the surface as a function of the w/c ratio. d = days; S = 10% silica fume.





**FIGURE 16.** Relative strength at water curing (strength at water curing to strength at sealed curing), 50 mm from the surface as a function of the w/c ratio. d = days; S = 10% silica fume.

was included in the concrete composition, the strength rose by only about 20% at the surface of a normal concrete due to water curing. At a lower w/c ratio or at 150 mm or 350 mm distance from the surface, the difference in strength from the strength of a sealed specimen was minor. Compared to the results of the cube test, an opposite result was obtained in this case. This was due to the size of the specimen. The 150-mm cube probably developed wet conditions at the surface only, but the cylinder core probably got wet through during the water curing. Water-cured cubes obtained stresses due to the curing conditions, which decreased the strength [4].

## Split Tensile Strength

The variation in the compressive strength due to distance from the cured surface and due to the curing condition (sealed, air, or water) was analyzed earlier. In Figure 19, the results of the split tensile strength at sealed curing are shown as a function of the compressive strength at sealed curing. Two cores were used to obtain the compressive strength for each core used for the split strength. The compressive strength cores were geometrically taken close to the split tensile strength cores in the large specimens. Figure 19 includes results from 216 cores [1,5]. The age of the concrete is indicated. In Figures 20 and 21, the split tensile strength at air curing and water curing is given as a function of the

compressive strength. Figures 20 and 21 include results from 216 cores each [1,5]. The age of the concrete is indicated. In Figures 22, 23, and 24, the split tensile strength at constant age during sealed curing, air curing, and water curing is given as a function of the compressive strength. Figures 22, 23, and 24 include results from 216 cores each [1,5]. The kind of curing is indicated in the figures.

## Analysis of Split Tensile Strength

From Figure 19, the following time-dependent relationship was obtained for split tensile strength,  $f_{ct}$ , at sealed curing (MPa):

$$f_{ct} = 0.23 \times e^{-0.00041t} \times f_{cc}^{(0.785 + 0.000061t)} \{R^2 = 0.91\} \quad (8)$$

where  $f_{cc}$  is the compressive strength (MPa),  $t$  is the age of concrete (days), and  $R^2$  is the coefficient of variation.

The long-term split tensile strength decreased slightly compared with the compressive strength during sealed curing. Both at air curing and at water curing, a significant decrease of the split tensile strength after 450 days was observed in Figure 20 and Figure 21. However, at both 28 and 90 days of age, the split tensile strength was fairly independent of the kind of curing (Figures 22 and 23). In Figure 24, it was observed that the split tensile strength decreased at both air curing and water curing

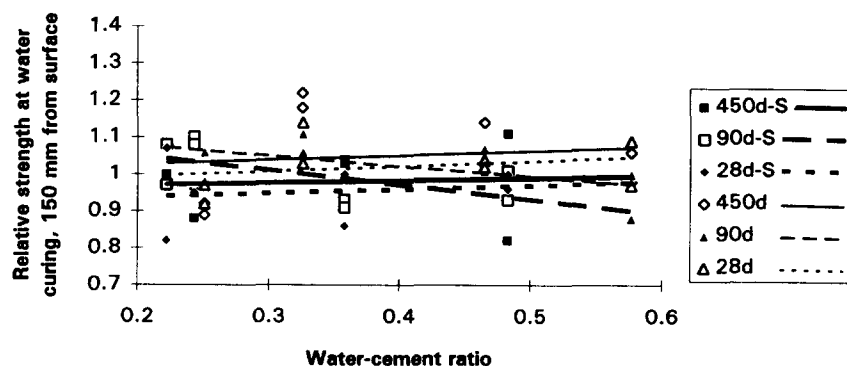


**FIGURE 17.** Relative strength at water curing, 150 mm from the surface as a function of the w/c ratio. d = days; S = 10% silica fume.

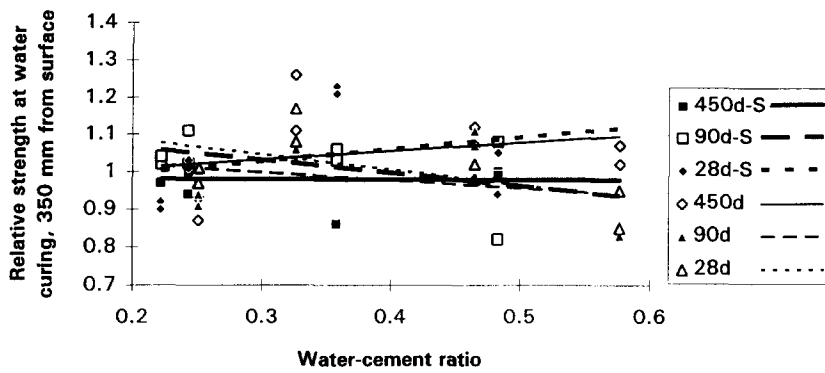


FIGURE 18. Relative strength at water curing, 350 mm from the surface as a function of the w/c ratio. d = days; S = 10% silica fume.

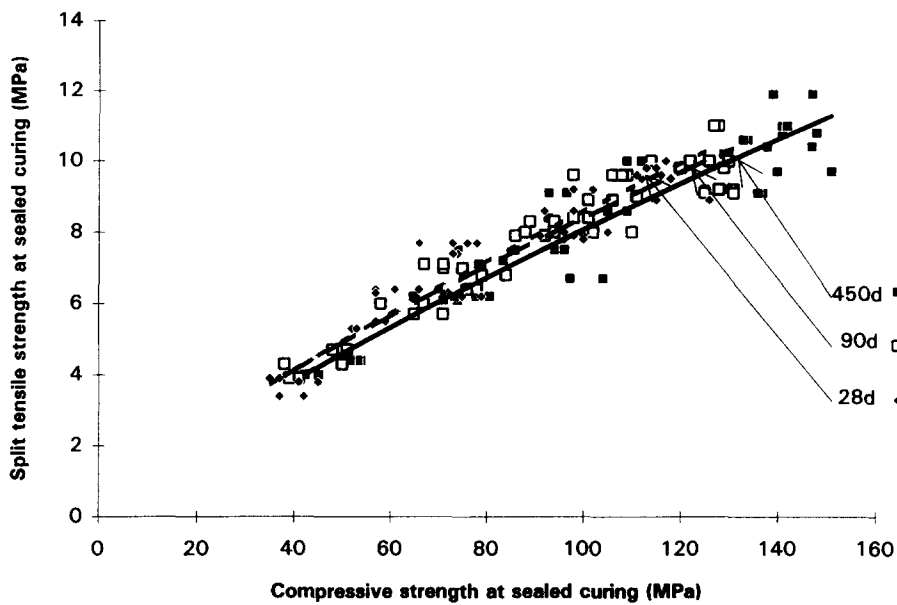


FIGURE 19. Split tensile strength as function of compressive strength at sealed curing. The age of concrete is indicated. d = days.

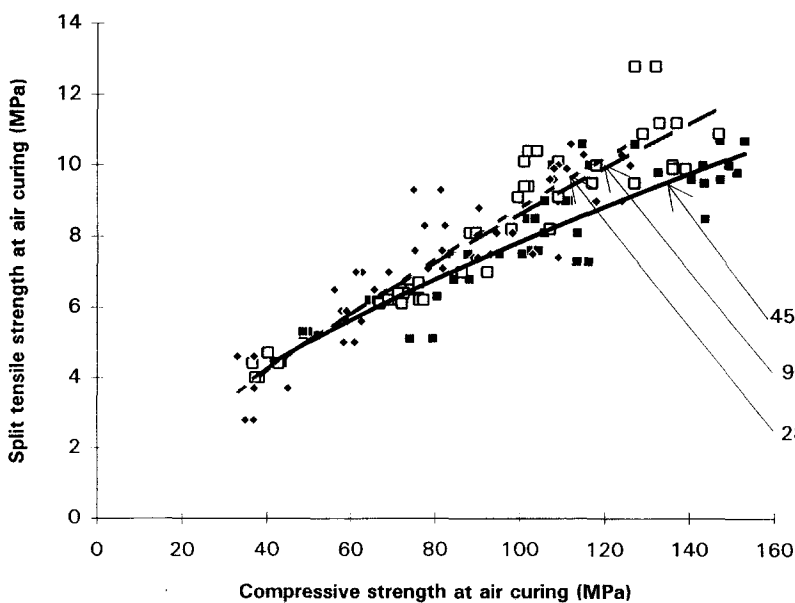


FIGURE 20. Split tensile strength at air curing as a function of the compressive strength. The age of the concrete is indicated. d = days.

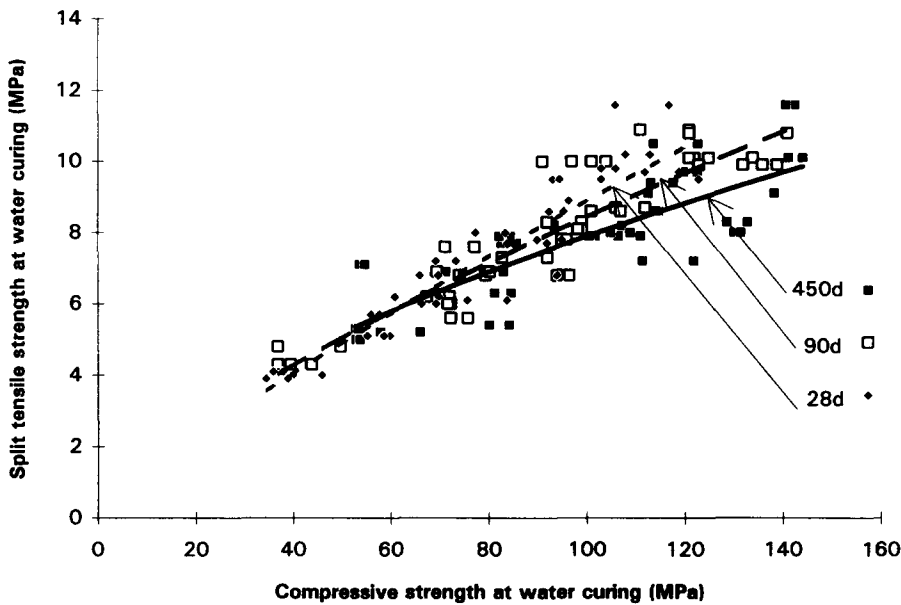


FIGURE 21. Split tensile strength at water curing as a function of the compressive strength. The age of the concrete is indicated. d = days.

compared with sealed curing. The following equations were obtained:

$$f_{ct,a} = 0.39 \times f_{cc}^{0.65} \quad \{R^2 = 0.86\} \quad (9)$$

$$f_{ct,s} = 0.19 \times f_{cc}^{0.81} \quad \{R^2 = 0.91\} \quad (10)$$

$$f_{ct,w} = 0.48 \times f_{cc}^{0.61} \quad \{R^2 = 0.71\} \quad (11)$$

where  $f_{ct,a}$  is the split tensile strength at 450 days age during air curing (MPa),  $f_{ct,s}$  is the split tensile strength at 450 days age during sealed curing (MPa),  $f_{ct,w}$  is the split tensile strength at 450 days age during water curing (MPa),  $f_{cc}$  is the compressive strength at 450 days

age during the same kind of curing (MPa), and  $R^2$  is the coefficient of variation.

The eq 11 exhibited a very low coefficient of variation. However, eq 9 and 11 were similar to equations obtained by Jaccoud [6] summarized according to:

$$f_{ct,sp} = 0.385 \times f_c^{0.6} \quad (12)$$

where  $f_{ct,sp}$  is the split tensile strength (MPa) and  $f_c$  is the compressive strength (MPa). The substantial decrease of the split tensile strength during air curing and water curing compared with sealed curing was due to the

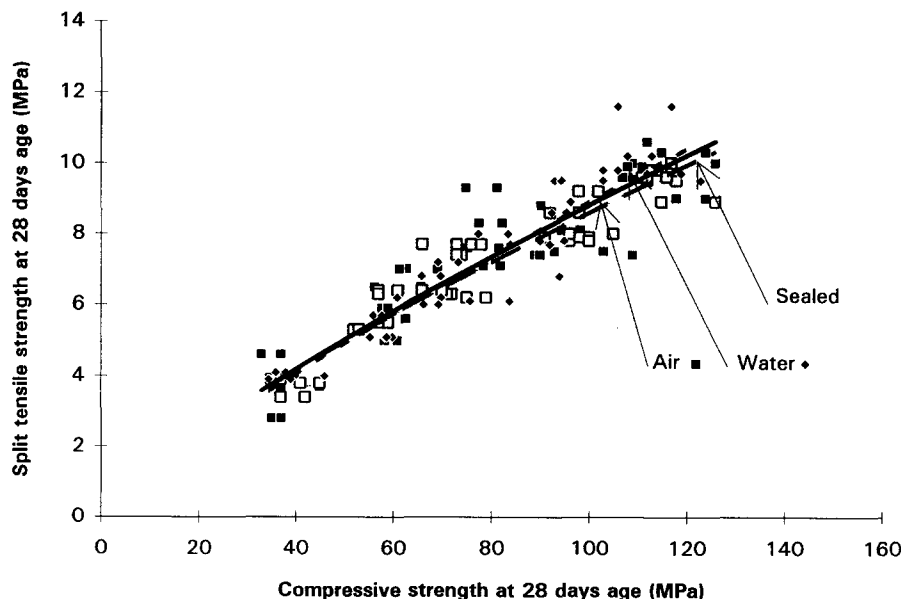


FIGURE 22. Split tensile strength at 28 days age as a function of the compressive strength. The kind of curing is indicated.

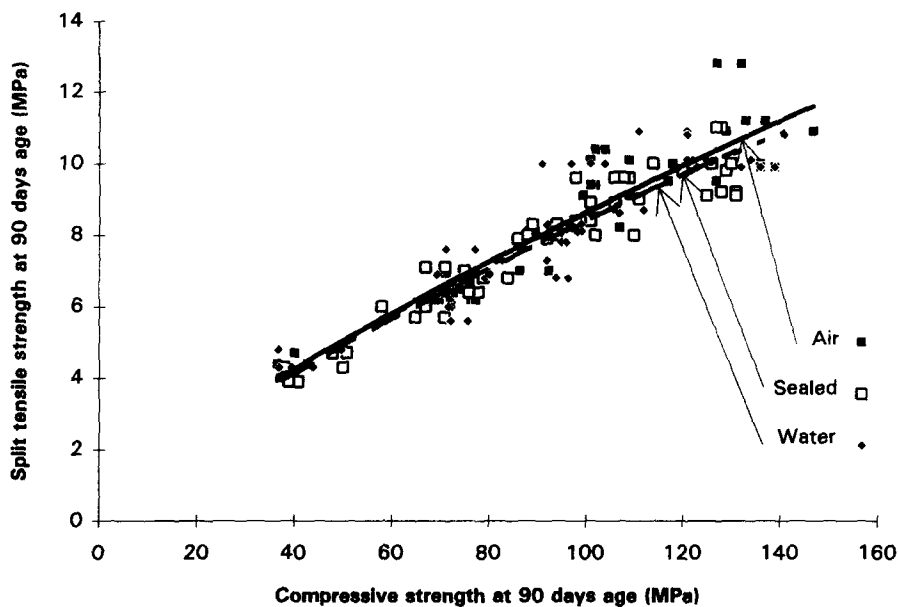


FIGURE 23. Split tensile strength at 90 days age as a function of the compressive strength. The kind of curing is indicated.

moisture conditions in the concrete. It was then of interest to study the difference in internal relative humidity between the sealed curing and air curing or water curing. As mentioned earlier, the internal relative humidity was measured at the same distance from the surface as where the cores were taken out from the large concrete specimens. In Figure 25, the relative split tensile strength (ratio of the split tensile strength at air curing or water curing to the split tensile strength at sealed curing) is given as a function of the difference between the internal relative humidity at sealed curing and at air curing or water curing [1,5]. The internal relative humidity of the concrete was compared at each

location of the drilled cores in the large specimens. However, only tendencies could be observed in Figure 25, because measurements both of split strength and internal relative humidity are hard to carry out. The preliminary conclusions of Figure 25 were: (1) the split tensile strength of HPC with silica fume was more sensitive to changes in the internal relative humidity than the split tensile strength of concrete without silica fume, and (2) the split tensile strength of concrete at a lower w/c ratio decreased more with changes in the internal relative humidity than the split tensile strength in normal concrete. More research is required to confirm these tendencies.

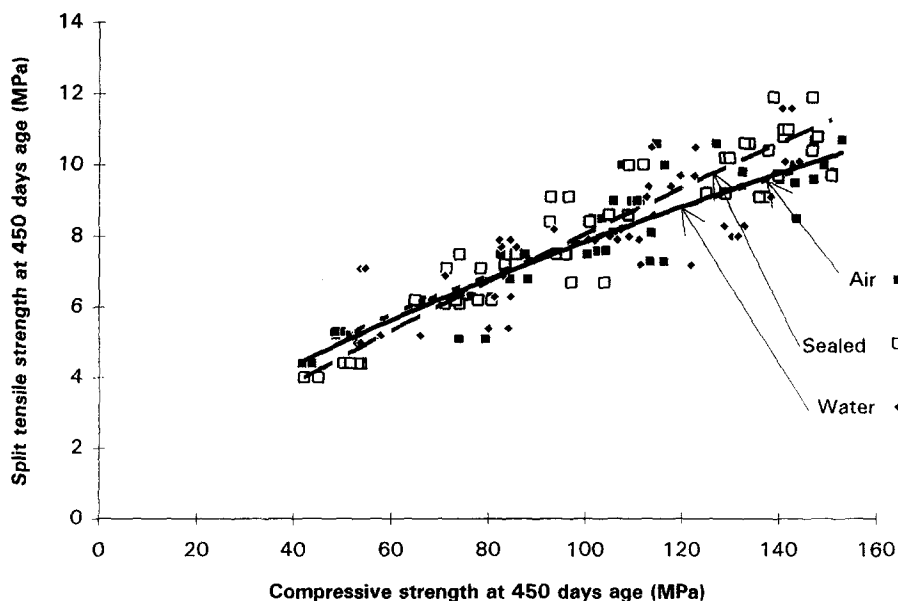
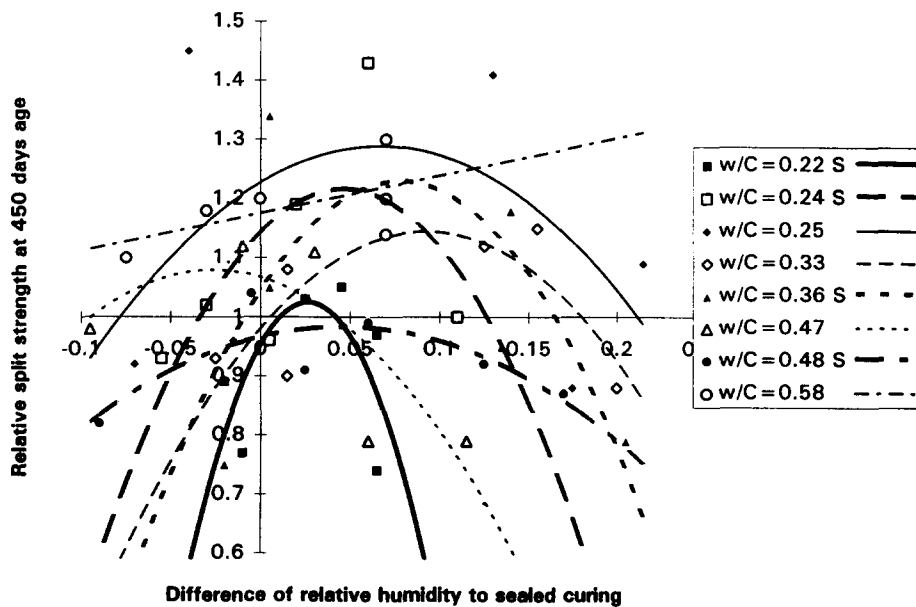


FIGURE 24. Split tensile strength at 450 days age as a function of the compressive strength. The kind of curing is indicated.



**FIGURE 25.** Relative split tensile strength as a function of the difference between the internal relative humidity at sealed curing and at air curing or water curing.

## Hydration

It was of interest to study to what extent the hydration of the concretes depended on the curing conditions and on the age. The influence on the content of silica fume in the concrete on the hydration was also of interest. All the 432 cylinders from the compressive strength tests were used as specimens (about 250 g concrete each). In all, the hydration of 110 kg concrete was studied. The fragments of the compressive test were further crushed into pieces of maximum of 5 mm concrete. The pieces were rapidly heated at 105°C in an oven for 1 week. After the drying of the evaporable water, the fragments were cooled in a exsiccator and weighed. The fragments

were then ignited at 1050°C for 16 hours and then cooled in an exsiccator before the final weighing was performed. The chemically bound water was obtained according to Byfors [7]:

$$\frac{w_n}{c} = \frac{w^{105}(1 - \eta) - w^{1050}}{w^{1050} - \frac{3 \times \gamma}{1 + \gamma} \times w^{105}} \quad (13)$$

where  $w_n/c$  is the ratio of nonevaporable water to amount of cement (kg/kg),  $w^{105}$  is the weight after drying at 105°C (kg),  $w^{1050}$  is the weight after ignition at 1050°C (kg), and  $\gamma$  is the ratio of aggregate to cement.

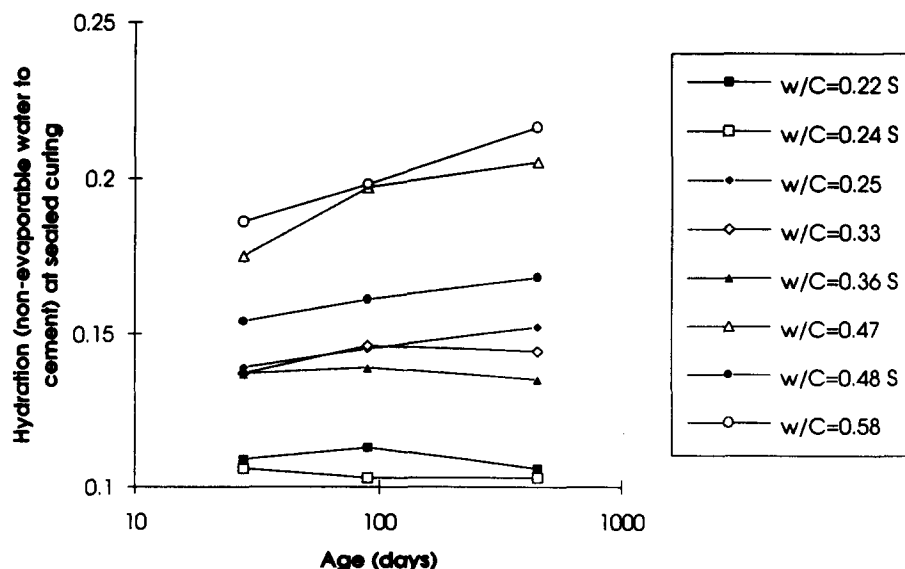


**FIGURE 26.** Hydration,  $w_n/c$ , as a function of logarithmic age at sealed curing (six measurements); w/c ratio (w/C) content is indicated. S = 10% silica fume.

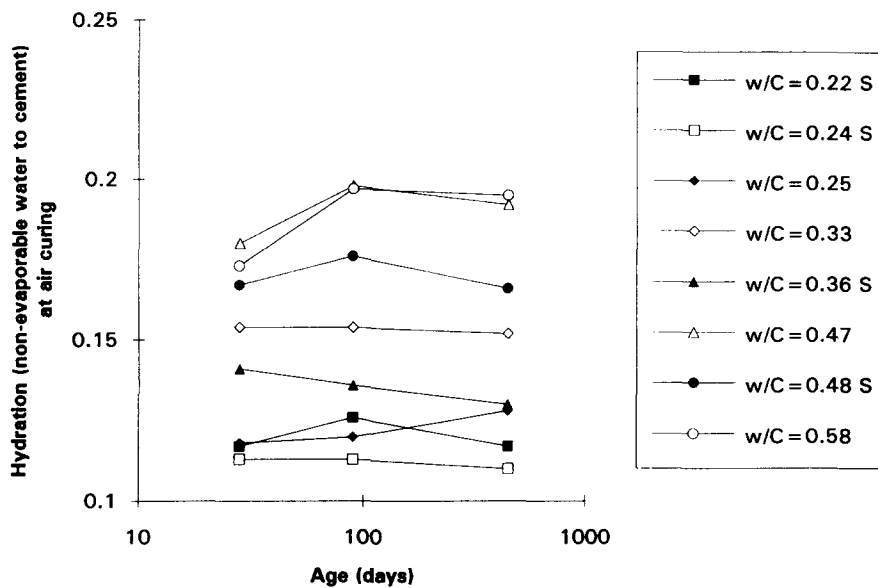


**FIGURE 27.** Hydration,  $w_n/c$ , as a function of logarithmic age at air curing (six measurements);  $w/c$  ratio ( $w/C$ ) is indicated. S = 10% silica fume.

$$\mathfrak{S} = 1 - \mu_a \quad (14)$$

$$\eta = \frac{\mu_c + \gamma \times \mu_a}{1 + \gamma} \quad (15)$$

where  $\mu_a$  is the ignition losses for aggregate (kg/kg) and  $\mu_c$  is the ignition losses for cement (kg/kg).

The distance from the cured surface (the edge of the rim), 50, 150, or 250 mm, had very little influence on the hydration [5]. This fact was probably explained by the large size of the specimen. Due to the small differences observed relating the distance to the surface, the mean value of the hydration of the measured distances was calculated including six measurements. In Figures 26, 27, and 28, the ratio of nonevaporable water to amount

of cement,  $w_n/c$ , is given as a function of logarithmic age for sealed curing, air curing, and water curing. In Figures 26, 27, and 28, the ratio of nonevaporable water to amount of cement,  $w_n/c$ , developed differently, depending on the presence of silica fume. As the silica fume reacted with the calcium hydroxide in the concrete, the nonevaporable water to amount of cement,  $w_n/c$ , dropped after 90 days, most probably due to polymerization [8].

## Discussion of Hydration and Strength

No strength decline was observed during the 450 days. The compressive strength increased for concretes sub-

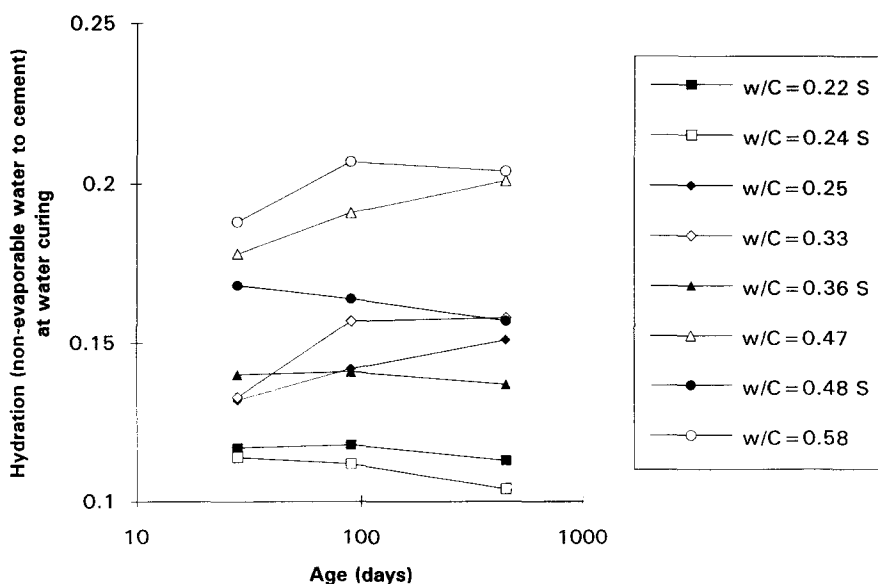


**FIGURE 28.** Hydration,  $w_n/c$ , as a function of logarithmic age at water curing (six measurements)  $w/c$  ratio ( $w/C$ ) and content of silica fume is indicated.

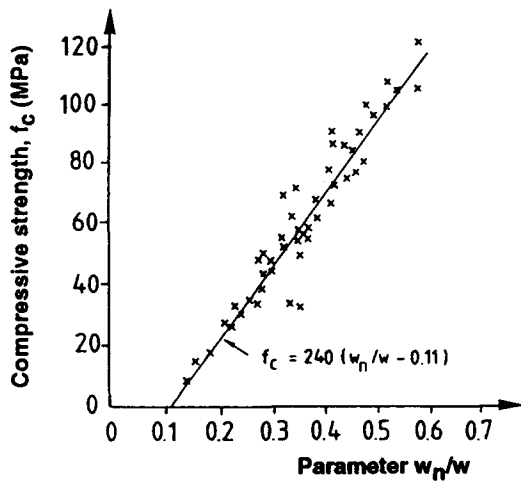


FIGURE 29. Compressive strength,  $f_c$ , of 50 mm cement-paste cubes as a function of the relative strength,  $w_n/w$ . Low-alkali cement [9].

jected to both air and water curing and also during sealed curing conditions. The split tensile strength followed the increase of the compressive strength fairly well at sealed curing. At higher strength, the increase of split strength at sealed curing was less pronounced, probably due to the properties of the aggregate (split tensile strength of aggregate = 15 MPa). At 450 days, a decrease of the split tensile strength of HPC was observed at both air curing and water curing, most probably due to moisture-related stresses between the aggregate and the cement paste. However, it is normally assumed that the hydration of the concrete (expressed as the ratio of nonevaporable water to the cement,  $w_n/c$ ) increases with the strength of the concrete. This was not

the case in this study in concretes that contained silica fume. An HPC contains less water than is necessary for the hydration to proceed to a final state of  $w_n/c \approx 0.25$ . The maximum degree of hydration,  $\alpha = 1$ , can then only be obtained at a  $w/c$  ratio larger than 0.39. The maximum degree of hydration,  $\alpha$ , of a curing with a  $w/c$  ratio less than 0.39 is then linear dependent on the  $w/c$  ratio [5]:

$$\alpha_{\max} = \frac{w}{0.39 \times c} \quad (16)$$

where  $w$  is the mixing water of the concrete ( $\text{kg}/\text{m}^3$ ) and  $c$  is the cement content of the concrete ( $\text{kg}/\text{m}^3$ ). The degree of hydration,  $\alpha$ , can also be expressed as:

$$\alpha = \frac{w_n}{0.25 \times c} \quad (17)$$

where  $w_n$  is the nonevaporable water content of the concrete ( $\text{kg}/\text{m}^3$ ) and  $c$  is the cement content of the concrete ( $\text{kg}/\text{m}^3$ ). Dividing eq 16 by 17 gave the maximum value of the relative hydration defined as:

$$(w_n/w)_{\max} = 0.64 \{0 < w/c < 0.39\} \quad (18)$$

$$(w_n/w)_{\max} = 0.25 \times c/w \{w/c > 0.39\} \quad (19)$$

where  $w_n$  is the nonevaporable water content of the concrete ( $\text{kg}/\text{m}^3$ ),  $w$  is the mixing water of the concrete ( $\text{kg}/\text{m}^3$ ), and  $c$  is the cement content of the concrete ( $\text{kg}/\text{m}^3$ ).

In Figure 29, the relationship between the relative hydration,  $w_n/w$ , and the compressive strength,  $f_c$ , of a

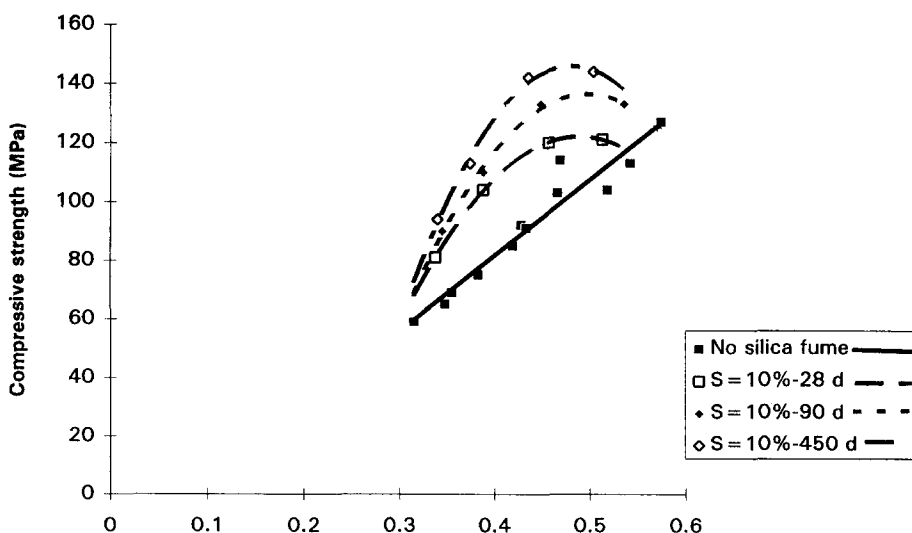


FIGURE 30. Compressive strength,  $f_c$ , of concrete cylinders as a function of the relative hydration,  $w_n/w$ . Content of silica fume is indicated in the figure. d = days.

low-alkali cement paste is given [9]. The strength was obtained for cube 50 × 50 mm. Recalculation into 40-mm diameter cylinders (80 mm in length) [5] gave the compressive cylinder strength,  $f_{c,cyl}$  (MPa) as a function of the relative hydration (ratio of nonevaporable water to cement),  $w_n/w$ :

$$f_{c,cyl} = 210 \times (w_n/w - 0.135) \quad \{\text{No silica fume; } R^2 = 0.83\} \quad (20)$$

It was reasonable to believe that a relationship would also exist between the relative hydration  $w_n/w$  and the compressive strength of HPC. In Figure 30, the compressive strength of all the cylinders tested in the work (432 cylinders) is shown as a function of the relative hydration.

The following equation applied for the compressive cylinder strength,  $f_{c,cyl}$ , of concrete without silica fume (MPa) as a function of the ratio of the relative hydration (nonevaporable water to cement),  $w_n/w$ :

$$f_{c,cyl} = 260 \times (w_n/w - 0.085) \quad \{\text{No silica fume; } R^2 = 0.93\} \quad (21)$$

However, for concrete with silica fume, the relative hydration,  $w_n/w$ , declined after 90 days age in spite of the increase in strength of the concrete. The following equation applied for the compressive cylinder strength,  $f_{c,cyl}$ , of concrete with 10% silica fume (MPa) as a function of the ratio of the relative hydration (nonevaporable water to cement),  $w_n/w$ :

$$f_{c,cyl} = 310 \times \{\ln t \times [0.030 - (w_n/w - 0.46)^2] - 2.25 \times (w_n/w - 0.54)^2 + 0.31\} \quad \{10\% \text{ silica fume; } R^2 = 0.97\} \quad (22)$$

The following symbols applied in eqs 20, 21, and 22:  $f_{c,cyl}$  is the compressive strength of cylinder of 40 mm diameter and 80 mm length (MPa),  $t$  is age (days),  $w_n$  is the nonevaporable water content of the concrete (kg/m<sup>3</sup>),  $w$  is the mixing water of the concrete (kg/m<sup>3</sup>), and  $R^2$  is the coefficient of variation.

## Conclusions

The long-term development of internal relative humidity, strength, and hydration was studied for eight concretes during sealed curing, air curing, or water curing at 28, 90, and 450 days. The w/c ratio of the concrete varied between 0.22 and 0.58. Half of the concretes contained 10% silica fume. The specimens consisted of 1 m diameter rims with a thickness of 100 mm. The flat sides of the large specimen were sealed by epoxy plastic resin. The large specimen simulated a column with a diameter of 1 m.

The internal relative humidity was measured with a total of 144 cast-in plastic pipes 50, 150, or 350 mm from the circular edge of the rim. The sealed curing exhibited a remarkable self-desiccation, especially when silica fume was utilized in the composition of the concrete. Even at water curing, the internal relative humidity in a concrete with a w/c ratio of 0.22 dropped to 0.8 after 450 days of curing as close as 50 mm to the water-cured surface. The self-desiccation of concrete was found to be dependent on time and the w/c ratio.

To obtain the strength, a total of 648 cores were drilled out of the rims. The strength of the concrete increased continuously during the 450 days independent of the kind of curing. The strength development was also fairly independent of the distance from the cured edge of the rim to the core (50, 150, or 250 mm). The strength was affected only in concrete of higher w/c ratio by the kind of curing. Another equation indicated that the so-called efficiency factor between silica fume and cement content, as referred to the compressive strength of 432 cores, varied between 1 and 8 due to the age and the w/c ratio of the concrete. As a result, the strength developed more slowly for concretes containing silica fume than for concretes without silica fume content. Still, the strength of concretes with silica fume increased at least over 450 days. Relationships were obtained between compressive and split tensile strength including 648 specimens. At 450 days, the split tensile strength was lower related to the compressive strength at both air and water curing than at sealed curing, most probably due to self-stresses created by the moisture differences in the concrete.

The self-desiccation affected the hydration process. For concrete without silica fume, the degree of hydration increased continuously. For concretes with silica fume, however, the degree of hydration decreased after an age of approximately 90 days. Finally, expressions were also found between the strength of the concrete and the development of the relative hydration (ratio of the hydrated water and the mixing water content in the concrete).

## References

1. Persson, B. *Hydration, Structure, and Strength of High Performance Concrete. Data and Estimations*, Report TVBM-7011. LTH Building Materials: Lund, Sweden, 1992.
2. Hassanzadeh, M. *Fracture Mechanical Properties of High Performance Concrete*, Report M4:05. LTH Building Materials: Lund, Sweden, 1994; p. 27.
3. ASTM. *Standard Practice for Maintaining Constant Relative Humidity by Means of Aqueous Solutions*, ASTM E 104-85. The American Society for Testing and Materials: Philadelphia, 1985.
4. Atlasi, E. *Effect of Moisture on the Compressive Strength of High Performance Concrete*. Proceedings at the Symposium of High-Strength Concrete, Lillehammer, Norway, 1993.



5. Persson, B. *Hydration, Structure, and Strength of High Performance Concrete*, Licentiate Thesis. Report TVBM-1009. LTH Building Materials: Lund, Sweden; 1992.
6. Wittmann, F.H.; Schwesinger, P. *High Performance Concrete: Material Properties and Design*. Proceedings of the Fourth Weimar Workshop on High Performance Concrete: Material and Design held at Hochschule für Architektur und Bauwesen (HAB) Weimar, Germany, October 4th and 5th, 1995. AEDIFICATIO Verlag GmbH. D-79104 Freiburg i.Br. and CH-8103 Unterengstringen, 1995.
7. Byfors, J. *Plain Concrete at Early Ages*, Ph.D. thesis. Report FO 3:80. The Cement and Concrete Institute: Stockholm, Sweden, 1980.
8. Kühl, H. *Der Baustoff Zement*. Verlag für Bauwesen: Berlin, 1967; p. 211.
9. Powers, T.C.; Brownnyard, T.L. *Studies of Physical Properties of Hardened Portland Cement Paste*, Research Laboratories of the Portland Cement Association. Bulletin 22, Vol. 43. Journal of the American Concrete Institute: Detroit MI, 1947.